THE MATHEMATICAL MODELS OF ELECTROCHEMICAL GRINDING FOR THE PRECISION PRODUCTION

SERGEY BRATAN[1], IVAN KURIC[2], BORIS YAKIMOVICH[1], UMER ABDULGAZIS[3], DILYAVER ABDULGAZIS[3]

[1]Sevastopol State University, Sevastopol, Crimea

[2]University of Zilina, Faculty of Mechanical Engineering, Department of Automation and Production Systems, Slovakia

[3]Crimean Engineering and Pedagogical University named after Fevzi Yakubov, Simferopol, Crimea

This article considers the development of a mathematical model of electrochemical grinding for processing precision components operating at varying loads. The combination of processes (for example, the mechanical and electrochemical material removal processes) significantly improves operation control capabilities by increasing the number of control inputs and selected input variables. The results of the research are presented as evaluated based on the capacity of products manufactured using this grinding method. The conducted qualitative and quantitative assessments demonstrate the adequacy of mathematical models. The difference between experimental and calculated values made up 5-10%. The electrochemical grinding helps improve the operability of components operating at varying loads compared to mechanical grinding.

1 INTRODUCTION

One of the key goals of mechanical engineering is to improve production processes based on complex automation and the development of automated production systems [Nemethova 2018 & 2019] and software-controlled equipment [Pokorny 2008, Kosinar 2011, Peterka 2020a]. This is especially relevant for the production of precision devices like accelerometers. The improvement of component processing efficiency for these devices is associated with the improved quality of surface processing [Peterka 2013]. These can only be achieved simultaneously by using new progressive processing methods and optimal production control [Reznikov 1977, Peterka 2020b]. Consider the technical requirements and implementation possibility of these aspects using an example of accelerometer rockers, which is a flat component featuring complex configuration and profiled surface made with Quality classes 5-6 and surface roughness Ra = 0.16–0.8 μm. Conventionally, the products of these quality classes were produced using diamond grinding processing [Yakimov 1977]. The grinding of DA-9 accelerometer rockers requires a large amount of finishing operations and requires high workmanship from individual workers. The consistency of finished component quality is 13-15% of all processed components with each component requiring 1-3 hours to produce. The analysis of publications [Podurayev 1977, Bratan 2006] shows that one of the key aspects of controlled processing development is combined grinding in passivation media. In this case, the combination of processes significantly improves operation control capabilities by increasing the number of control inputs and selected input variables [Nikitin 2020, Peterka 2020c]. This formation method provides high processing precision (Quality classes 5-6) and low surface roughness (Ra = 0,16 um), lacks the majority of disadvantages typical of other finishing methods, and is the most efficient for the formation of precision surfaces. However, the further expansion of the application areas of this method is restricted by the lack of adequate physical and mathematical models. Thus, the purpose of this research work is to develop the mathematical models of surplus removal during combined grinding in passivation media.

The problem with developing a rational control strategy is associated with the complexity of the physical processes involved in surface formation due to a large number of technological factors that can be used to change the parameters of this process.

2 DESIGN OF MATHEMATICAL MODELS

To produce a mathematical model for the calculation of material removal during anode-mechanical grinding, consider the interaction of the abrasive tool and the workpiece on the micro level when the electric field affects the processed surface and forms passivation films on it [Kuric 2022]. In the analysis, we consider the roughness of the surface formed during previous working runs. During the combined grinding, material removal can occur due to the anodic dissolution of the processed metal Q_A, workpiece surface micro-cutting with tool grains Q_M, metal removal due to electrical erosion Q_E, and a combination of these processes.

We can write the resulting subtraction in the form (1):

$$Q_\Sigma = Q_A + Q_M + Q_E \qquad (1)$$

We know that the anodic dissolution of metals during anode-mechanical grinding is discrete in each local area of the anode surface. Because of this, the usage of impulse voltage does not improve the processing parameters compared to process voltage [Podurayev 1977]. Thus, in the analysis, we consider the impacts of direct current on the workpiece surface.

Considering the design features of the research object, we selected plunge-cut grinding. This system stipulates that the processed surface can contact the grinding disk continuously. We know that an electrical field in passivation media like liquid glass or water solutions of NaNO3, Na2SO4, etc. leads to the formation of insoluble, high-impedance passivation films on the surface of the workpiece (anode) for the majority of metals and alloys, e.g., steels, beryllium bronzes, brasses, titanium, etc, which leads to the rate reduction (deceleration) of anodic dissolution of the metal from the maximum to zero. After the complete passivation with so-called Flade potential, the anodic dissolution of metal stops completely [Podurayev 1977]. The rate of anodic dissolution of metal in passivation media is in an exponential relationship with the processing time (see Fig. 1) and can be determined using the following expression:

$$Q(\tau) = c \times e^{-\alpha(t-\tau)}, \qquad (2)$$

where c is the instant linear rate of anodic metal dissolution, t is the given moment in time, τ is the workpiece surface activation time, α is the passivation coefficient.
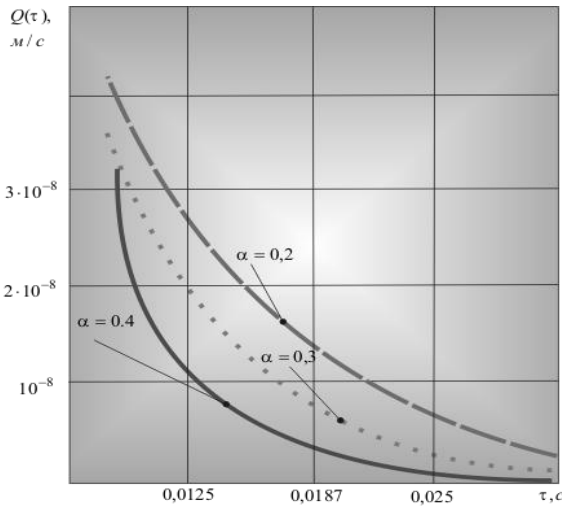
Figure 1. The dependency between anodic dissolution rate and processing time in passivation media

Multiplying expression (2) by S_n and Dt, we get the removal caused by anodic metal dissolution on the elementary area:

$$\Delta Q_{(V)} = Q(\tau) \cdot S_n = S_n \cdot c \cdot \Delta t \cdot \exp[-\alpha(t - \tau)], \quad (3)$$

where S_n is the surface area of the elementary area.

The local linear rate of anodic metal dissolution, in turn, can be calculated using the dependency [Podurayev 1977]:

$$c = \varepsilon_{\ni} \times i \times \eta, \quad (4)$$

$$\varepsilon_{\ni} = \frac{100}{\sum \dfrac{c_j}{\varepsilon_j}}$$

Where $\dfrac{}{\varepsilon_j}$ is the linear electrochemical equivalent of the alloy, c_j is the percentage content of a specific component in the alloy, ε_j is the electrochemical equivalent of the component, i is the current density, η is the current output.

In anode-mechanical grinding, passivation is accompanied by abrasive tool impacts. The cutting of the elementary area ΔN with the abrasive grains results in the local activation of the anodic surface, i.e., the elementary area gets an active zone after an abrasive grain pass, which results in the reduced polarization and the redistribution of voltage drop between the anodic area and the electrolyte layer. The negative shift of the potential activates metal dissolution but hampers other processes on the anode that require greater polarization values. This is manifested in the local current output increase η. Active dissolution lasts several uses and depends on the electrolyte composition and processed component material. The current density in the active zone (the area is cut) increases and drops in the passive zone (the area is not cut) due to the redistribution of equipotential and power lines of the electric field (see Fig. 2) that occurs due to the differences of anodic potentials in these zones. In this case, side reactions in the passive zone are reduced. Therefore, even when using passivation electrolytes, the total current output is close to one. For the same reason, as electrode voltage increases, the current output increases too [Podurayev 1977]. Consider that the $\eta \to 1$ expression for the calculation of instant linear rate of anodic metal dissolution can be written down as $c = \varepsilon_{\ni} i$. Assume that the real process is in line with the Ohm's law.
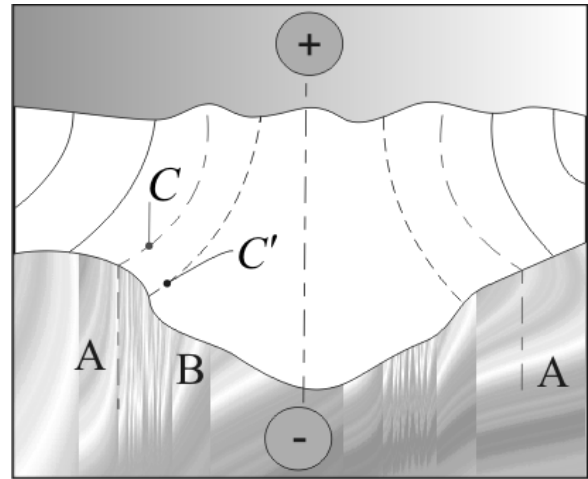

Figure 2. The redistribution of power lines, A is the active anodic dissolution zone, B is the passive anodic dissolution zone, C are power lines in the active zone, C' are power lines in the passive zone

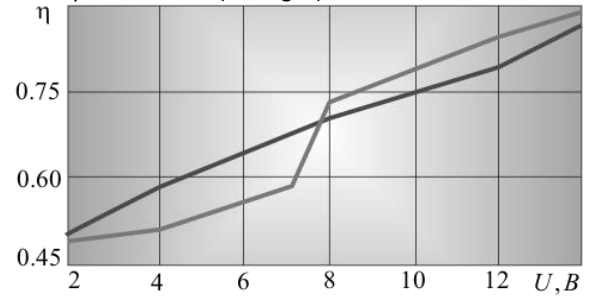These patterns are confirmed by the experimental processing of beryllium bronzes (see Fig. 4).

Figure 3. The dependency between the current output U on the electrodes for beryllium bronze and 30KhN2MFA steel components (non-considering the abrasive impact)

current in the electrolyte loop can be calculated using the known dependency:

$$I = \frac{z \times u}{\delta} = \frac{u}{R_3} \quad (5)$$

where u is the loop voltage drop, R_3 is the impedance of the interelectrode gap, δ is the interelectrode gap, z is the conductivity of the electrolyte.

Research [Podurayev 1977] presents an expression to calculate electric conductivity considering gas production:

$$z = z_0 \exp{-\frac{R \cdot T_{\ni} \cdot z_0 \cdot D}{2 F_{\Phi} \cdot V \cdot \rho_{\ni}^2}} \quad (6)$$

where R is the universal gas constant, $T_{\ni}$ is the electrolyte temperature, D is the factor accounting for hydrogen pressure in gas bubbles, F_{ϕ} is the Faraday constant, $\rho_{\ni}$ is the gas density, z_0 is the specific electrolyte conductivity.

Based on the above, the expression for metal removal with anodic dissolution on the elementary area can be written down as:

$$\Delta Q(\tau') = \frac{\varepsilon_{\ni} \cdot u \cdot z_0 \cdot S_n \cdot \Delta t}{\delta} \exp[-x - \alpha(t - \tau)], \quad (7)$$

where $x = \dfrac{R \cdot T_{\ni} \cdot z_0 \cdot D}{2 F_{\Phi} \cdot V \cdot \rho_{\ni}^2}$, $\Delta Q(\tau')$ is the metal dissolution rate on the elementary area.

After an abrasive grain pass, the processed surface forms an elementary area. If we know the number of areas ΔN that occur at any given moment, we can calculate:

$$\Delta Q_{\Theta X} = \left[\Delta Q(\tau') \cdot S_n \cdot \Delta N(\tau)\right] \cdot \Delta t \tag{8}$$

where ΔN is the number of areas and Δt is the time increment. The only unknown value in equation (2) is ΔN, i.e., the number of areas occurring at any given moment. To obtain a dependency that can be used for the calculation of the number of areas that occur at any given moment t, review Figure 5.
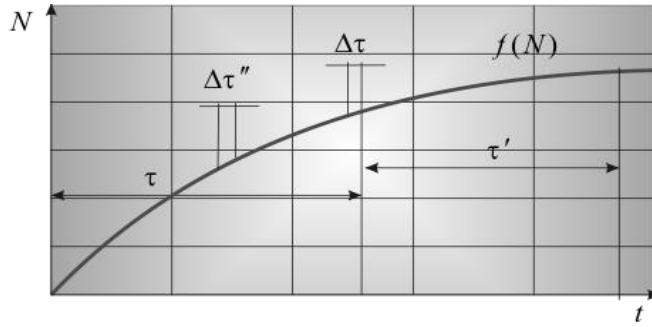

Figure 5. The flowchart for the calculation of the electrochemical removal of metal considering surface renewal due to abrasive impacts

Assume that at the moment t_0 the workpiece level in question is processed by the tips of the protruding abrasive grains.

When abrasive grains contact the surface of the metal, elementary areas occur there. However, as individual cuts overlap, the majority of grains have incomplete contact with the material. It does not span the entire width of the abrasive grain. Other abrasive grains only experience individual risks. In this case, areas are not formed.

The number of grains contacting the material is proportional to the probability of its non-removal. Thus, by analyzing the probability of grain tips contacting the material, we can calculate the number of areas formed at the moment τ. The probability of such area occurrence is equal to the probability of gain profile passing through the metal. For instance, if, during Dτ, level Δu located within $u = 0$ to $u = t_\phi$ is passed by $\Delta\lambda$ grains, the number of areas occurred is:

$$P_n = \Delta\lambda \cdot P(\overline{M}) \tag{9}$$

where $P(\overline{M})$ is the probability of material non-removal at τ at the level *W*.

However, some of the areas formed at τ꘡enter the processing zone of one of the grains considering the overlap and can be cut at any moment:

$$\tau' = t - \tau \tag{10}$$

where t is the given moment in time, τ' is the area existence time.

To determine the number of areas at any moment t, we need to multiply the formation probability of the area P_n by the probability of the area formed during $\Delta\tau$ at the level W not being cut.

$$\Delta N(\tau') = \Delta\lambda \cdot P(\overline{M}) \cdot P_N(\overline{M}) \tag{11}$$

where $P_N(\overline{M})$ is the probability of the area formed during $\Delta\tau$ at the level W not being cut.

The number of grains passing through the section W during $\Delta\tau$ can be calculated based on the distribution density

$$\Delta\lambda_{\Delta\tau} = V_K \cdot n_3 \cdot f(u) \cdot \Delta u \cdot \Delta\tau \tag{12}$$

where n_3 is the number of grains in the volume unit of the working layer of the tool, u is the distance from the simulated external surface of the tool to the grain tip, and V_k is the peripheral speed of the tool.

By approximating the distribution function of the working grain number $f(u)$ using the power dependence $\dfrac{\chi}{H_u^{\chi}} u^{\chi-1}$, we get:

$$\Delta\lambda = \left[V_k \cdot n_3 \int_0^W \frac{x}{H_u^{x}} u^{x-1} du \right] \Delta\tau \tag{13}$$

where H_u is the thickness of the working layer of the disk used for the calculation of the abrasive grain number n_3, χ is the power index.

After integration on u, dependency (4) looks as follows:

$$\Delta\lambda = \frac{V_k \cdot n_3 \cdot W^x}{H_u^{x}} \cdot \Delta\tau \tag{14}$$

The probability of the material not being removed at τ at the level W is determined with the following dependency:

$$P(\overline{M}) = \exp\left[-a(y;\tau)\right] \tag{15}$$

where $a(y;\tau)$ is the sum of grain cross-sections at the level W over the period from t_0 to τ is determined using the expression:

$$a(y;\tau) = k_C \cdot b_3(y) \cdot \lambda \tag{16}$$

where k_c is the chip formation factor, λ is the number of grains passing through an individual section, $b_3(y) = \dfrac{\overline{b}_{31} + \overline{b}_{32} + ... + \overline{b}_{3n}}{n}$ is the width of abrasive grain profiles.

When the grain profile is approximated with a power dependency (a rotational paraboloid in the simplest case)

$$\overline{b}_3(y) = c_b \left[t_\phi - y - u \right]^m \tag{17}$$

where C_b, m are grain shape factors, y is the distance from the external surface of the workpiece to the level in question.

Over $\Delta\tau''$, the workpiece surface is passed by a section with an arc length of $V_k \cdot \Delta\tau''$.

Of the total number of grains that pass through the section, the profile width $\overline{b}_3(y)$ can be observed in the grains whose tips are in the disk layer $1 \cdot \Delta u \cdot V_K \cdot \Delta\tau''$. The number of these tips can be calculated using the distribution density $f(u)$.

$$\Delta\lambda = n_3 \cdot V_K \cdot f(u) \cdot \Delta u \cdot \Delta\tau''$$

(18)

After the respective substitutions, we get an expression for the calculation of $\Delta a(y;\tau)$:

$$\Delta a(y;\tau) = k_C \cdot n_3 \cdot V_K \cdot C_b [t_\phi - y - u]^m \cdot f(u) \cdot \Delta u \cdot \Delta\tau''$$

(19).

During the steady-state anode-mechanical grinding, the component size changes continuously and in proportion to the processing time. In the surface section located at a distance y from the base plane, the material starts to be removed at t_0 when the tips of the protruding grains start passing through the level in question. The material can be removed completely when the grain leaves the contact area.

Shifting from a discrete model to a continuous one, we get an integral equation that determines the changes in the probability parameter in the contact zone between the workpiece and the disk at τ at the level W:

$$a(y;\tau) = n_3 \cdot V_k \cdot k_c \int_{t_0}^{\tau} \int_0^{S_y \cdot \tau''} b_3 \cdot f(u) \cdot du \cdot d\tau''$$

(20)

Having approximated the distribution function $f(u)$ with a power dependency and after the integration on u and τ, we get:

$$a(y;\tau) = \frac{x \cdot k_c \cdot C_b \cdot \Gamma(m+1) \cdot \Gamma(x) \cdot n_3 \cdot V_k \cdot [S_y(\tau - t_0)]^{x+m+1}}{H_u{}^x \cdot (m+x+1) \cdot \Gamma(x+m+1) \cdot S_y},$$

(21)

where $\Gamma(m+1); \Gamma(\chi); \Gamma(x+m+1)$ are the values of G functions; S_y is the speed of the working tool surface in the workpiece material in the feed direction.

Denote the following:

$$A = \frac{x \cdot k_c \cdot C_b \cdot \Gamma(m+1) \cdot \Gamma(x) \cdot n_3 \cdot V_k}{H_u{}^x \cdot (x+m+1) \cdot \Gamma(x+m+1)},$$

(22)

$$Q = AS_y{}^{x+m}$$

(23)

Since t_0 is the moment when the first grain passes through a level, the calculation formula for $a(y;\tau)$ looks as follows:

$$a(y;\tau) = A \cdot S_y{}^{x+m} \cdot \tau^{x+m+1}$$

(24)

By substituting (7) in (6) we get an expression (8) for the calculation of material non-removal probability at τ at the level W.

$$P(\overline{M}) = \exp[-Q\tau^{x+m+1}]$$

(25)

The probability $P_N(\overline{M})$ of the area formed at the level W over the time $\Delta\tau$ not being cut during τ' can be calculated as follows:

$$P_N(\overline{M}) = \exp[-a(\tau')] = \exp[-a(t) - a(\tau)]$$

(26)

Having performed similar transformations, we get an integral equation that can determine the changes in the sum of grain cross sections at the level W over τ',

$$a(t) = \int_{\tau}^{t} \int_0^{S_y \cdot \tau'''} b_3 \cdot f(u) \cdot d\tau'''$$

$$a(\tau) = \int_{t0}^{\tau} \int_0^{S_y \cdot \tau''} b_3 \cdot f(u) \cdot d\tau''$$

(27)

By using power dependencies for the approximation of abrasive grain profiles and the distribution function, after integration (10) we get:

$$a(t) = \frac{x \cdot k_c \cdot C_b \cdot \Gamma(m+1) \cdot \Gamma(x) \cdot n_3 \cdot V_k \cdot [S_y \cdot \tau']^{x+m+1}}{H_u{}^x (x+m+1)\Gamma(x+m+1)S_y},$$

$$a(\tau) = \frac{x \cdot k_c \cdot C_b \cdot \Gamma(m+1) \cdot \Gamma(x) \cdot n_3 \cdot V_k \cdot [S_y \cdot \tau]^{x+m+1}}{H_u{}^x \cdot (x+m+1)\Gamma \cdot (x+m+1) \cdot S_y}.$$

Denoting

$$\Theta = $$
$$\frac{x \cdot k_c \cdot C_b \cdot \Gamma(m+1) \cdot \Gamma(x) \cdot n_3 \cdot V_k \cdot S_y{}^{x+m+1}}{H_u{}^x \cdot (x+m+1) \cdot \Gamma(x+m+1) \cdot S_y},$$

(28)

we get an equation for the calculation of $a(\tau')$:

$$a(\tau') = a(t) - a(\tau) = \Theta \cdot t^{x+m+1} - \Theta \cdot \tau^{x+m+1}$$

(29)

After the substitution of (11) in (9), the calculation expression for the probability of the area formed over $\Delta\tau$ at the level W not being cut during τ' looks as follows:

$$P_N(\overline{M}) = \exp[-\Theta \cdot (t^{x+m+1} - \tau^{x+m+1})]$$

(30)

Substitute (5), (8), (12) in (3) and assume:

$$\Delta N(\tau') = \frac{V_k \cdot n_3 \cdot (S_y \cdot \tau)^x}{H_u{}^x} \Delta\tau \cdot \exp[-\Theta \cdot \tau^{x+m+1}] \cdot \exp[-\Theta \cdot (t^{x+m+1} - \tau^{x+m+1})]$$

(31)

Denote:
$$\frac{V_k n_3 S_y{}^x}{H_y{}^x} = G, \quad x+m+1 = K$$

In this case, the equation for the calculation of $\Delta N(\tau')$ considering the notations above can be written down as:

$$\Delta N(\tau') = G \cdot \tau^x \Delta\tau \cdot \exp(-\Theta \cdot t^K)$$

(32)

After the substitution of (1) and (13) in (2), the calculation dependency for the electrochemical metal removal increase taking into account surface renewal through abrasive impacts can be written down as follows:

$$\Delta Q_{ЭX} = S_n \cdot \Delta t \cdot c \cdot \exp(-\alpha(t-\tau)) \cdot G \cdot \tau^x \Delta\tau \cdot \exp(-\Theta \cdot t^K)$$

(33)

Denote $S_n \cdot \Delta t \cdot c \cdot G = L$, then

$$\Delta Q_{ЭX} = L \cdot \tau^x \cdot \exp(-\alpha(t-\tau)) \cdot \exp(-\Theta \cdot t^K) \cdot \Delta\tau = L \cdot \tau^x \cdot \exp(-\alpha t + \alpha\tau - \Theta \cdot t^K) \cdot \Delta\tau$$

(34)

After the integration of expression (14) on τ, we get an integral equation that describes electrochemical metal removal taking into account surface renewal due to abrasive impacts.

$$Q_{\Im X} = L \cdot \int_0^t \tau^x \exp(\alpha\tau - \alpha t - \Theta t^K) \cdot d\tau \qquad (35)$$

Further integration is only possible when the values of parameters x and K are known. With $x = 1.5, K = 3$, expression (15) looks as follows:

$$Q_{\Im X} = L \int_0^t \tau^{1,5} e^{\alpha\tau - \alpha t - \Theta t^3} dt.$$

$$Q_{\Im X} = L \cdot \int_0^t \tau^{1,5} \exp(\alpha\tau - \alpha t - \Theta t^3) \cdot d\tau \qquad (36)$$

Equation (16) can be used to calculate the electrochemical removal of material taking into account workpiece surface renewal due to the abrasive impacts in any point of the contact zone between the disk and the workpiece and trace the area cutting patterns with individual abrasive grains.

3   APPLICATION OF MATHEMATICAL MODELS

Example: Calculate $Q_{\Im x}$ when grinding copper workpieces.

Grinding mode:
- the peripheral speed of the tool $V_k = 5 m/s$;
- the speed of the tool in the feed direction $S_y = 10^{-6}$ ms,
- current density $i = 10$ A/cm2, $K_C = 0.9$,
- $\rho_s = 21 \times 10^{-6} m$, $n_3 = 5.2 \times 10^6$ 1/m^2 for disks with a granularity of 250 um,
- electrochemical copper equivalent $\varepsilon_h = 0,021$ mm/A·min.

The calculation can be performed with:

$H_u = 10.87 \times 10^{-6} M$, $\Delta\tau = 1c$, $\alpha = 0.,8$, $t = 1c.$

Calculate the integral using numerical integration, and search interval 0;3.
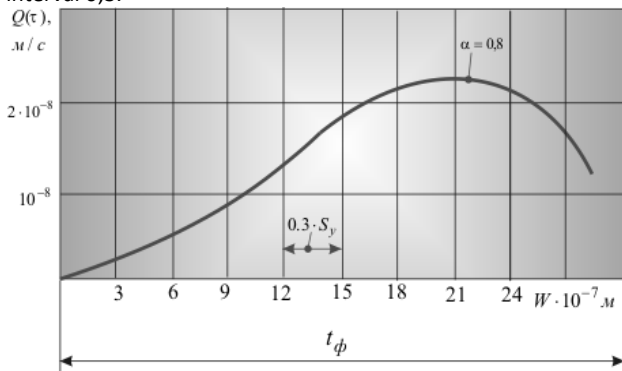

Figure 6. The dependency between metal removal speed in the contact zone levels within the actual cutting depth

The calculation data (see Figure 6) show that when passing the disk/workpiece contact zone, the rate of metal removal is increased within the actual cutting depth to a specific level, reaches maximum, and is then reduced as it approaches the level corresponding with t_ϕ; then approaches zero. Based on this calculation, we can assume that during the first contact of the disk and the workpiece (at the moment t_0), the material starts to be removed. In this case, the number of operating cutting edges is greater than the number of areas formed. Therefore, the number of areas formed initially will be increasing. After several disk/workpiece contact instances, the number of the disk's cutting edges in operation will be balanced by the number of elementary areas formed and will then be reduced. Thus, the number of formed elementary areas on the surface of the workpiece will reach a maximum and then be reduced, until the number of areas approaches zero at the depth of $\geq t_\phi$.

The electrochemical removal of the material taking into account surface renewal due to abrasive impacts is affected by all of the grinding modes. As they change, the slope of the ascending and descending branches of the curve changes as well, along with the length and position of the maximum (see Figure 7). Increasing disk speed and workpiece passivation degree, as well as maximum cutting depth reduction result in the reduction of curve lengths, and their maximum shifts toward smaller values of W.

With $\alpha = 0$, i.e., when there is no passivation, the electrochemical removal of metal $Q_{\Im x}$ reaches a maximum value for the grinding modes in question.

$$Q_{\Im X\alpha} = L \int_o^t \tau^{1.5} e^{-\Theta \cdot t^3} dt \qquad (37)$$

The obtained data show that the removal of metal is significantly affected by passivation that occurs during anode-mechanical grinding. As the passivation capacity of the electrolyte increases, the rate of electrochemical removal is reduced, and processing precision is increased. When there is no passivation, the workpiece surface is etched along the grain borders. To simplify the calculations of $Q_{\Im x}$, introduce K_N those accounts for the impact of passivation on the electrochemical removal of the metal taking into account surface renewal due to abrasive impacts.

$$K_N = \int_o^t \tau^{1.5} \exp(-\alpha \cdot t + \alpha \cdot \tau - \Theta \cdot t3) d\tau / \int_o^t \tau^{1.5} \exp(-\Theta \cdot t3) dt \qquad (38)$$

In this case, the expression describing the rate of electrochemical material removal taking into account surface renewal with abrasive impacts looks as follows:

$$Q_{\Im X} = \frac{\varepsilon_\Im \cdot i \cdot \eta \cdot K_N}{6 \cdot 10^{-2}} = B \cdot K_N \qquad (39)$$

The rate of material removal with mechanical cutting can be calculated based on the evaluation of the shift of the equal probability of metal removal before and after the contact of the workpiece surface section and the tool [Novoselov 1979].
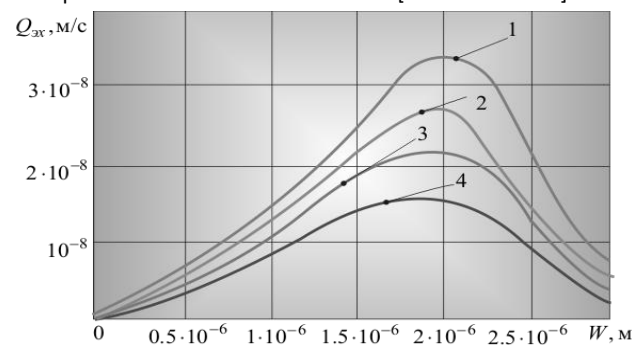

Figure 7. The dependency between metal removal rate Q$_{EH}$ and the mode parameters. Where for curve : $1 - \alpha = 0.1$, $2 - \alpha = 0.4$, $3 - \alpha = 0.8$, $4 - \alpha = 1.2$

In the case of plunge-cut grinding, the dependency looks as follows:

$$P(M) = 1 - exp\left[\frac{\pi \cdot k_C \cdot \sqrt{2\rho_s} \cdot n_s \cdot V_k \cdot Sy^2 \cdot t^3}{8 \cdot H_u^{1.5}}\right], \qquad (40)$$

where ρ_3 is the grain tip rounding radius.

Thus, the rate of material removal with mechanical cutting is equal to the movement speed of the tool's working surface in the workpiece material in the feed direction. After some simple transformation of dependency (18), we get an expression that can be used for the calculation of material removal with mechanical cutting.

$$Q_{MEX} = \frac{\pi \cdot k_C \cdot n_3 \cdot V_k \cdot t_{\Phi}^3 \cdot \sqrt{2 \cdot \rho_3}}{25{,}296 \cdot H_u^{1.5}} \qquad (41)$$

Denote

$$A = \frac{\pi \cdot k_C \cdot n_3 \cdot V_k \cdot \sqrt{2 \cdot \rho_3}}{25{,}296 \cdot H_u^{1.5}}.$$

Summing up expressions (17) and (19), we get an equation for the calculation of the total material removal rate for plunge-cut anode-mechanical grinding:

$$Q_{\Sigma} = Bk_n + At_{\Phi}^3. \qquad (42)$$

The analysis of equation (20) shows that, compared to the standard abrasive processing, combined grinding can help improve the efficiency of processing by the value of the electrochemical removal taking into account the abrasive impacts. The analysis of equation (20) shows that, compared to the standard abrasive processing, combined grinding can help improve the efficiency of processing by the value of the electrochemical removal taking into account the abrasive impacts.

Figure 8 Shows the dependency between the rate of material removal $Q_{\Sigma}, \text{м/с}$ and the medium passivation degree α and the tool feed $S_y, \text{m/s}$ at $I = 5\text{A/cm2}$, $V_u = 0.5\text{m/s}$, $\Delta\,O\,\otimes$ are the experimental data.
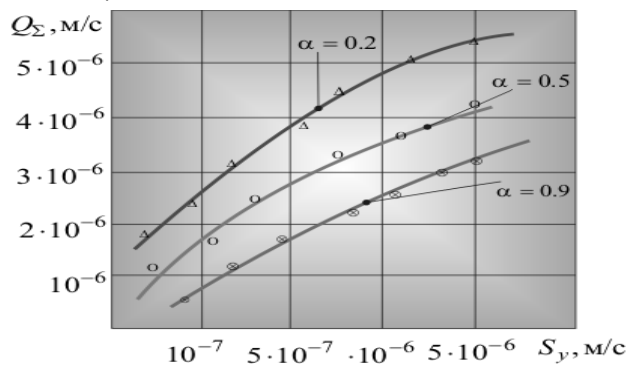
Figure 8. The dependency between the rate of material removal and the medium passivation degree

The adequacy of the produced mathematical model was evaluated by comparing the calculated and experimental data using specially developed equipment (see Figure 9 a, b, c).

The material removal was evaluated using a BIM-5 microscope as the average difference between the diameter and doubled indentation depth h after processing, measured in two perpendicular directions. The measurement error is ±0.0005 mm. The relative error of the calculated and experimental data does not exceed 15%, which indicates sufficient adequacy of the developed models.

To assess the operability of products after electrochemical grinding, they were compared with workpieces processed with mechanical grinding, which is the most popular finishing method for device components. To this end, we designed and produced a special setup (low-frequency relaxer) shown in Figure 10.
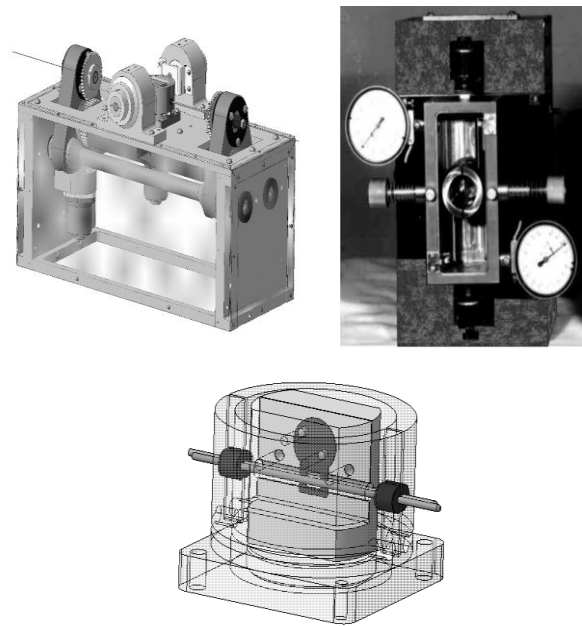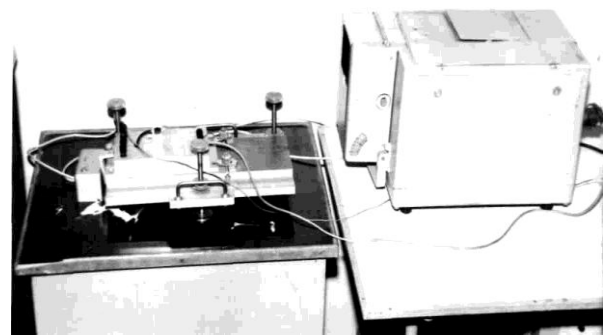
Figure 9. The specially developed equipment

Figure 10. Low-frequency relaxer

For comparative tests, we used DA-9 accelerometer rockers bade of BrB2 and 36KhNYu-VI steel with the same surface roughness of Ra=0.16.

The operability of components was determined using their durability. Durability was viewed as a result of random factors, i.e., as a random value. The number of cycles before destruction D was assumed as a random value [Hu 2022].

To test this, we experimented with two batches of samples made of beryllium bronze BrB2 and 36KhNYu-VI steel that underwent grinding under the following modes:

Batch 1: $U = 3\,\text{в}$, $S_y = 5 \cdot 10^{-6}\,\text{m/s}$, $V_k = 1{,}5\,\text{m/s}$, (following the X-ray research, this mode formed compressive residual stress in the surface layer of workpieces) [Bratan 2006];

Batch 2: $U = 3\,\text{в}$, $S_y = 10^{-6}\,\text{m/s}$, $V_k = 1{,}5\,\text{m/s}$ (residual stresses in the surface layer of workpieces are insignificant) [Bratan 2006];

Batch 3: obtained with the mechanical grinding of the materials in question: $U = 0\,\text{в}$, $S_y = 3 \cdot 10^{-6}\,\text{m/s}$, $V_k = 1{,}5\,\text{m/s}$ [5 Bratan 2006].

The samples were subjected to cyclic loads until their destruction.

We used the experimental data to develop sample distribution laws (Figure 11).

The analysis of Figure 11 shows that the stability of parameter D for workpieces that underwent electrochemical grinding is significantly higher than the stability of parameter D that

underwent mechanical grinding. The stability of this parameter is higher in the workpieces that do not have residual stresses in the surface layer.
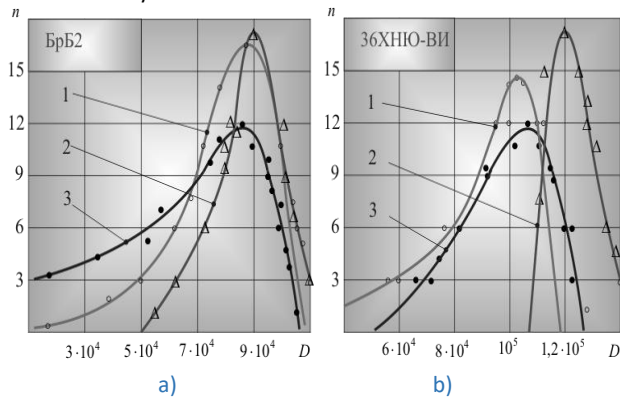

Figure 11. The distribution laws for samples, a) made of BrB2, b) made of 36KhNYuF-VI steel

Thus, the electrochemical grinding of device components helps significantly improve the durability.

4 CONCLUSIONS

1. The conducted qualitative and quantitative assessments demonstrate the adequacy of mathematical models. The difference between experimental and calculated values made up 5-10%. This helps use these models to control process parameters in a wide variation range during the grinding of various materials.

2. The electrochemical grinding helps improve the operability of components operating at varying loads compared to mechanical grinding. The guaranteed durability values are higher in the products featuring compressive residual stresses in the surface layer.

3. The study of electrochemical grinding operations [Bratan 2006] shows that if the parameters, processing modes, and grinding cycle are selected properly after its adjustment, the required precision parameters and component surface roughness can normally be achieved from the start of the tool operation.

Tool wear results in grains on its surface becoming blunt and areas forming on their tips. This affects the quality of the processed surface. The said phenomena need to be accounted for during the development of the mathematical models of this process. The developed problem demonstrates the prospects of further development in this area.

REFERENCES

[Bratan 2006] Bratan, S.M. The technological bases of quality assurance and stability increase for high-efficiency finishing grinding: author's abstract of the doctoral degree thesis in engineering. Machine Building Technology by S.M. Bratan. Odesa, 2006, 35 p.

[Hu 2022] Hu, J., et al. Autonomous dynamic line-scan continuous-wave terahertz non-destructive inspection system combined with unsupervised exposure fusion. NDT & E International 2022, 132. DOI: 10.1016/j.ndteint.2022.102705

[Kosinar 2011] Kosinar, M. and Kuric, I. Monitoring possibilites of CNC machine tools accuracy. 1st International Conference on Quality and Innovation in Engineering and Management (QIEM), 2011. Quality and Innovation in Engineering and Management, pp. 115-118.

[Kuric 2022] Kuric, I. et al. Implementation of predictive models in industrial machines with proposed automatic adaptation algorithm. Applied Sciences, 2022, Vol. 12, No. 4. DOI: 10.3390/app12041853.

[Nemeth 2018] Nemeth, M. and Peterkova, A. Proposal of data acquisition method for industrial processes in automotive industry for data analysis according to Industry 4.0. In: Book Series: IEEE Intern. Conf. on Intellig. Engineering Systems, 2018, pp. 157-161.

[Nemeth 2019] Nemeth, M., Nemethova, A. and Michalconok, G. Determination issues of data mining process of failures in the production systems. In: Book Series: Advance in Intelligent Systems and Computing 2019, 985, pp. 200-207.

[Nikitin 2020] Nikitin, Y., Bozek, P. and Peterka, J. Logical-Linguistic Model of Diagnostics of Electric Drive with Sensors Support. Sensors, 2020, Vol. 20, No. 16.

[Novoselov 1979] Novoselov, Yu.K. The surface formation dynamics during abrasive grinding. Saratov: Saratov University, 1979. 232 p.

[Pokorny 2008] Pokorny, P., Peterka, J. and Vaclav, S. The task of 5-axis milling. Technical Gazette, 2008, Vol. 19, No. 1, pp. 147-150.

[Peterka 2020a] Peterka, J. Nikitin, Y. and Bozek, P. Diagnostics of automated technological devices. MM Science Journal, 2020, pp. 4027-4034.

[Peterka 2013] Peterka, J., Pokorny, P. Influence of the Lead Angle from the Vertical Axis Milling on Radius of the Cutter. In: VII, 7th Int. Congress of Precision Machining (ICPM 2013), 2013, pp. 44-49.

[Peterka 2020b] Peterka, J. et al. Design and manufacturing of cutting tools for milling. MM Science Journal, 2020, No. March, pp. 3818-3821.

[Peterka 2020c] Peterka, J. et. al. Modification of Cutting tools by drag finishing. MM Science Journal 2020, pp. 3822-3825.

[Podurayev 1977] Podurayev, V.N. Automatically-controlled and combined cutting. Moscow: Mashinostroyeniye, 1977, 304 p.

[Reznikov 1977] Reznikov, A.N. Grinding and diamond processing of materials. Handbook. Moscow: Mashinostroyeniye, 1977, 380 p.

[Yakimov 1975] Yakimov, A.V. The optimization of grinding. Moscow: Mashinostroyeniye, 1975, 176 p.

CONTACTS:

Prof. Dr. Eng. Bratan Sergey
Sevastopol State University, Automation and engineering technology department
Universitetskaya 33, Sevastopol, Crimea, 299053, +79787155019, serg.bratan@gmail.com

Prof. Dr. Eng. Ivan Kuric
University of Zilina, Faculty of Mechanical Engineering, Department of Automation and Production Systems
Univerzitna 1, 010 26 Zilina, Slovakia, +421907418508, ivan.kuric@fstroj.uniza.sk

Prof. Boris A. Yakimovich
Sevastopol State University, Energy systems and complexes of traditional and renewable sources department
Universitetskaya 33, Sevastopol, Crimea, 299053, +79128542128, BAYakimovich@sevsu.ru

Prof. Dr. Eng. Umer Abdulgazis
Crimean Engineering and Pedagogical University named after Fevzi Yakubov, Motor transport department
Uchebniy alley 8, Simferopol, Crimea, 295015, +79787667918, at@kipu-rc.ru

Candidate of Eng. Sc. Dilyaver Abdulgazis
Crimean Engineering and Pedagogical University named after Fevzi Yakubov, Labor protection in mechanical engineering and social sphere department
Uchebniy alley 8, Simferopol, Crimea, 295015, +79782253725, ot@kipu-rc.ru